Supplementary materials

Supplementary methods

Description of simple ErbB-PHLDA1 model

We developed simple mathematical models, including ErbB2/HRGR dimer and tetramer formation and receptor phosphorylation, in which PHLDA1 hypothetically inhibits receptor phosphorylation and/or oligomerization. In detail, HRG directly binds to HRGR, and activates the receptor through the following steps; dimerization with ErbB2, phosphorylation, and tetramer formation (1). We considered the presence of ErbB2/HRGR dimer before HRG stimulation (pre-dimer) because Hiroshima et al., previously suggested that the presence of the pre-dimer (2). The inhibitory effect of PHLDA1 is hypothesized as occurring at either step of ErbB receptor activation in order to predict the molecular function of PHLDA1. We simplified in a way that ErbB receptor activation directly induces PHLDA1 production in order to focus on the effect of PHLDA1. All biochemical reactions in the model were described by ordinary differential equations (Tables S1 to S5).

Simulation method for cell-to-cell variability

Cell-to-cell variability was defined as the difference in protein abundance in individual cells. Simulations was performed by sampling initial protein concentration from the log-normal distribution of each protein with various coefficient of variation (CV). CVs of HRGR, ErbB2, ERK, Akt, and PHLDA1 were set to the experimental values measured in the MCF-7 cell line (Fig 3D), while CVs of other proteins were set to typical values (Tables S3 and S8). In addition, correlations between proteins, that is, PHLDA1-HRGR, PHLDA1-ErbB2, PHLDA1-ERK and PHLDA1-Akt, were obtained from the experimental data of the MCF-7 cell line (Fig 3G). Therefore, the initial concentrations of HRGR, ErbB2, ERK, Akt and PHLDA1 were randomly generated from those correlations (Tables S4 and S9). We performed 10,000 simulations each for simple and full models on cell-to-cell variability, and calculated the averaged dynamics, distributions at several time points, and Spearman's rank correlations among signaling proteins. We used CV of ErbB3 and correlation between PHLDA1-ErbB3 as substitutes for those of HRGR.

Description of expanded ErbB-PHLDA1 model

To develop a detailed mathematical model of the ErbB-PHLDA1 signaling network, we considered two major sub-networks, (1) the ErbB receptor signaling network including Ras-ERK and PI3K-Akt pathways and (2) the transcription regulatory network for PHLDA1 expression. Descriptions of these sub-networks were based both on the literature and our experiments using the MCF-7 cell line.

(1) ErbB receptor signaling network including Ras-ERK and PI3K-Akt pathways

HRG directly binds to HRGR at monomer and heterodimer, and activates ErbB receptors through phosphorylation in the MCF-7 cell line (3, 4). Ligand-activated ErbB receptors induce Ras-ERK and PI3K-Akt signaling (5, 6). Several mathematical models of these signaling pathways were previously published (4, 7-9). We constructed a novel mathematical model of the ErbB-PHLDA1 signaling network based on those published models (expanded model). In the full model, Ras-ERK signaling begins with the activation of Ras by ErbB receptors, then Ras activates Raf, MEK and ERK in turn (Fig. 5A). Active ERK phosphorylates and activates RSK, and both phosphorylated ERK and RSK promote the expression of c-Fos (10). In addition, DUSP induced by phosphorylated ERK rapidly dephosphorylates ERK (10). PI3K-Akt signaling also begins with activation of PI3K by ErbB receptors. Active PI3K phosphorylates PIP3, PDK1 and Akt in turn, then phosphorylated Akt carries out transcriptional regulation. All signaling proteins in both pathways are dephosphorylated by specific phosphatases (Fig. 5A).

(2) Transcription regulatory network for PHLDA1 expression

Earlier publications showed that PHLDA1 expression is mediated by either ERK or Akt pathways (11, 12). However, our studies with MEK (U0126) and Akt inhibitors showed that PHLDA1 expression was under control of both ERK and Akt pathways (Fig 1B and 1C). In addition, CHX treatment abolished PHLDA1 mRNA expression, suggesting that *de novo* synthesis of transcription factors is necessary prior to PHLDA1 expression (Fig. 1D). c-Fos is one of the transcription factors specifically induced in response to HRG (13), and the siRNA knockdown experiments showed weak inhibition of PHLDA1 expression (Fig. 1E). Based on these results, we estimated that PHLDA1 is transcriptionally regulated by both c-Fos and Akt pathways in the full model (Fig. 5A). Moreover, our experimental and mathematical analysis indicated that PHLDA1 inhibits

dimer and tetramer formation between ErbB receptors (Figs. 2 and 4). Therefore, a similar inhibition mechanism of PHLDA1 to ErbB receptors described in model M4 was represented in full model (Figs. 4A and 5A).

All biochemical reactions in the full model were described by ordinary differential equations (Table S2). This study used the evolutionary algorithm AGLSDC (14) to find the kinetic parameters that produce time-course consistent with our observations (Fig. 3B). All simulations in this study were implemented with XPPAUT (15).

Supplementary references

1. Zhang, Q., Park, E., Kani, K., and Landgraf, R. (2012) Functional isolation of activated and unilaterally phosphorylated heterodimers of ERBB2 and ERBB3 as scaffolds in ligand-dependent signaling. *Proc. Natl. Acad. Sci. USA*. 109, 13237–13242
2. Hiroshima, M., Saeki, Y., Okada-Hatakeyama, M., and Sako, Y. (2012) Dynamically varying interactions between heregulin and ErbB proteins detected by single-molecule analysis in living cells. *Proc. Natl. Acad. Sci. USA*. 109, 13984–13989
3. Nagashima, T., Shimodaira, H., Ide, K., Nakakuki, T., Tani, Y., Takahashi, K., Yumoto, N., and Hatakeyama, M. (2007) Quantitative transcriptional control of ErbB receptor signaling undergoes graded to biphasic response for cell differentiation. *J. Biol. Chem.* 282, 4045–4056
4. Birtwistle, M. R., Hatakeyama, M., Yumoto, N., Ogunnaike, B. A., Hoek, J. B., and Kholodenko, B. N. (2007) Ligand-dependent responses of the ErbB signaling network: experimental and modeling analyses. *Mol. Syst. Biol.* 3, 144
5. Yarden, Y., and Sliwkowski, M. X. (2001) Untangling the ErbB signalling network. *Nat. Rev. Mol. Cell Biol.* 2, 127–137
6. Holbro, T., Civenni, G., and Hynes, N. E. (2003) The ErbB receptors and their role in cancer progression. *Exp. Cell Res.* 284, 99–110
7. Hatakeyama, M., Kimura, S., Naka, T., Kawasaki, T., Yumoto, N., Ichikawa, M., Kim, J.-H., Saito, K., Saeki, M., Shirouzu, M., Yokoyama, S., and Konagaya, A. (2003) A computational model on the modulation of mitogen-activated protein kinase (MAPK) and Akt pathways in heregulin-induced ErbB signalling. *Biochem. J.* 373, 451–463
8. Borisov, N., Aksamitiene, E., Kiyatkin, A., Legewie, S., Berkhout, J., Maiwald, T., Kaimachnikov, N. P., Timmer, J., Hoek, J. B., and Kholodenko, B. N. (2009) Systems-level interactions between insulin-EGF networks amplify mitogenic signaling. *Mol. Syst. Biol.* 5, 256
9. Chen, W. W., Schoeberl, B., Jasper, P. J., Niepel, M., Nielsen, U. B., Lauffenburger, D. A., and Sorger, P. K. (2009) Input-output behavior of ErbB

signaling pathways as revealed by a mass action model trained against dynamic data. *Mol. Syst. Biol.* 5, 239

10. Nakakuki, T., Birtwistle, M. R., Saeki, Y., Yumoto, N., Ide, K., Nagashima, T., Brusch, L., Ogunnaike, B. A., Okada-Hatakeyama, M., and Kholodenko, B. N. (2010) Ligand-specific c-Fos expression emerges from the spatiotemporal control of ErbB network dynamics. *Cell*. 141, 884–896
11. Oberst, M. D., Beberman, S. J., Zhao, L., Yin, J. J., Ward, Y., and Kelly, K. (2008) TDAG51 is an ERK signaling target that opposes ERK-mediated HME16C mammary epithelial cell transformation. *BMC Cancer*. 8, 189
12. Kuhn, I., Bartholdi, M. F., Salamon, H., Feldman, R. I., Roth, R. A., and Johnson, P. H. (2001) Identification of AKT-regulated genes in inducible MERAkt cells. *Physiol. Genomics*. 7, 105–114
13. Saeki, Y., Endo, T., Ide, K., Nagashima, T., Yumoto, N., Toyoda, T., Suzuki, H., Hayashizaki, Y., Sakaki, Y., and Okada-Hatakeyama, M. (2009) Ligand-specific sequential regulation of transcription factors for differentiation of MCF-7 cells. *BMC Genomics*. 10, 545
14. Kimura, S., Nakakuki, T., Kirita, S., and Okada, M. (2011) AGLSDC: A Genetic Local Search Suitable for Parallel Computation. *SICE JCMSI*. 4, 105–113
15. Ermentrout, B. (2002) *Simulating, Analyzing, and Animating Dynamical Systems*, the Society for Industrial and Applied Mathematics

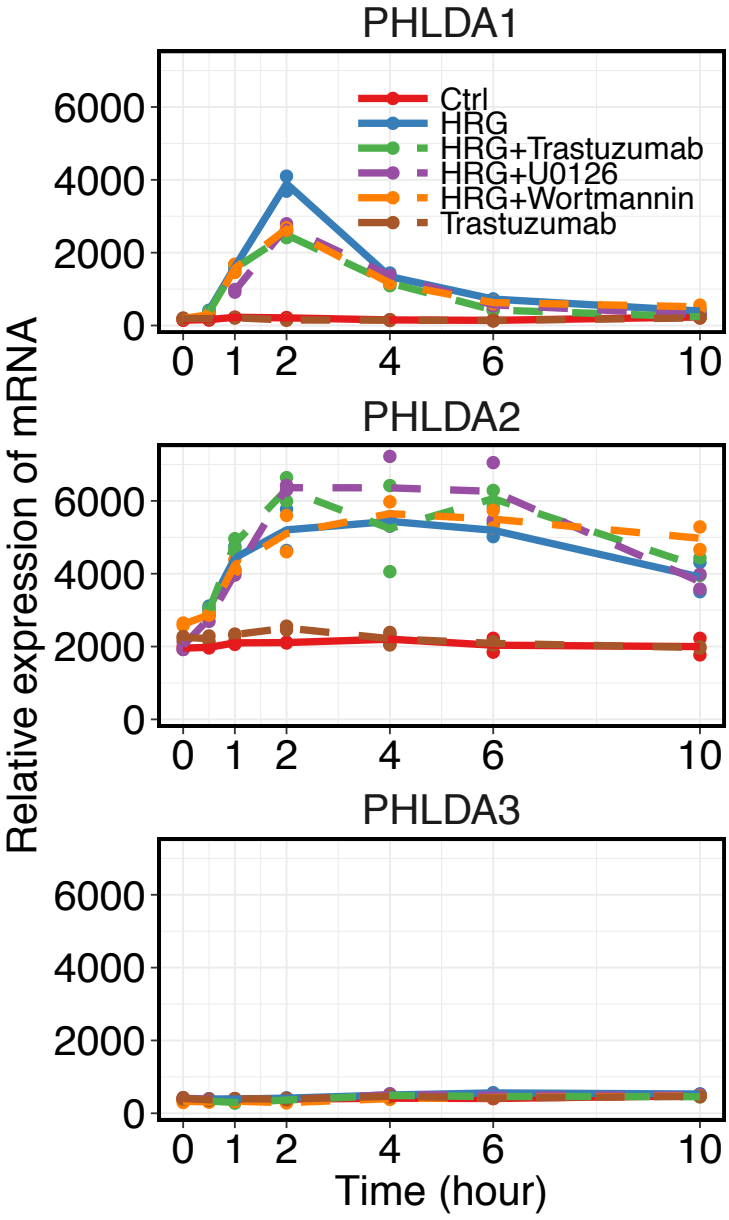

Fig. S1 *PHLDA1* gene family transcripts in HRG-stimulated MCF-7 cells (GSE13009, n = 2). The blue line shows the cells stimulated with HRG only and the red line shows unstimulated control. Trastuzumab (10 μg/ml, green line), U0126 (500 nM, purple), or wortmannin (100 nM, orange) was added 20 min prior to 10 nM of HRG stimulation. The brown line shows Trastuzumab-only treated condition.

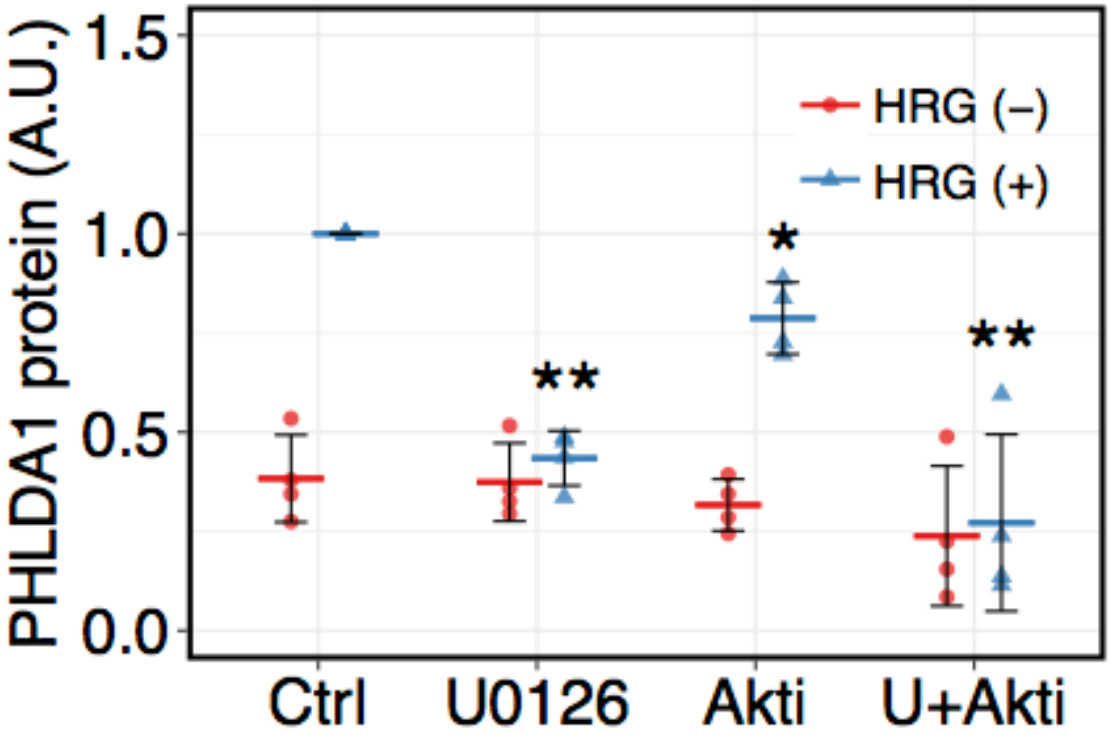

Fig. S2 Quantified value of the blot presented in Fig. 1C. The band intensities of PHLDA1 were quantified by dividing by that of α-tubulin, then the values were normalized so that the HRG-stimulated condition is designated as 1. Each point represents a result of an independent experiment, and colored bars mean average value of all experiments, and error bars denote standard deviation, n = 4. Two-tailed Welch's test was performed: *, $p < 0.05$; **, $p < 0.01$.

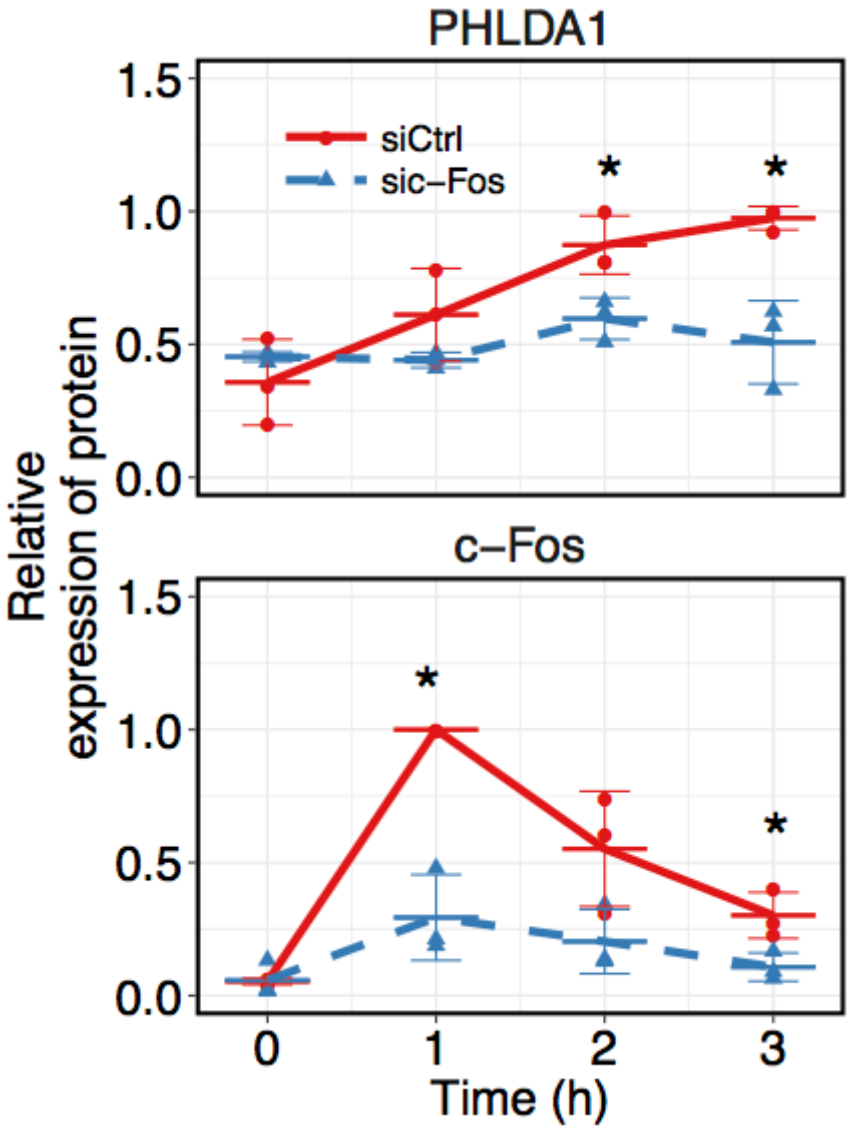

Fig. S3 Quantified value of the blot presented in Fig. 1F. The band intensities of PHLDA1 and c-Fos were quantified by dividing by that of α-tubulin, then the values were normalized so that the highest value in all conditions is designated as 1. Each point represents a result of an independent experiment, and colored bars mean average value of all experiments, and error bars denote standard deviation, n = 3. Two-tailed Welch's test was performed: *, $p < 0.05$.

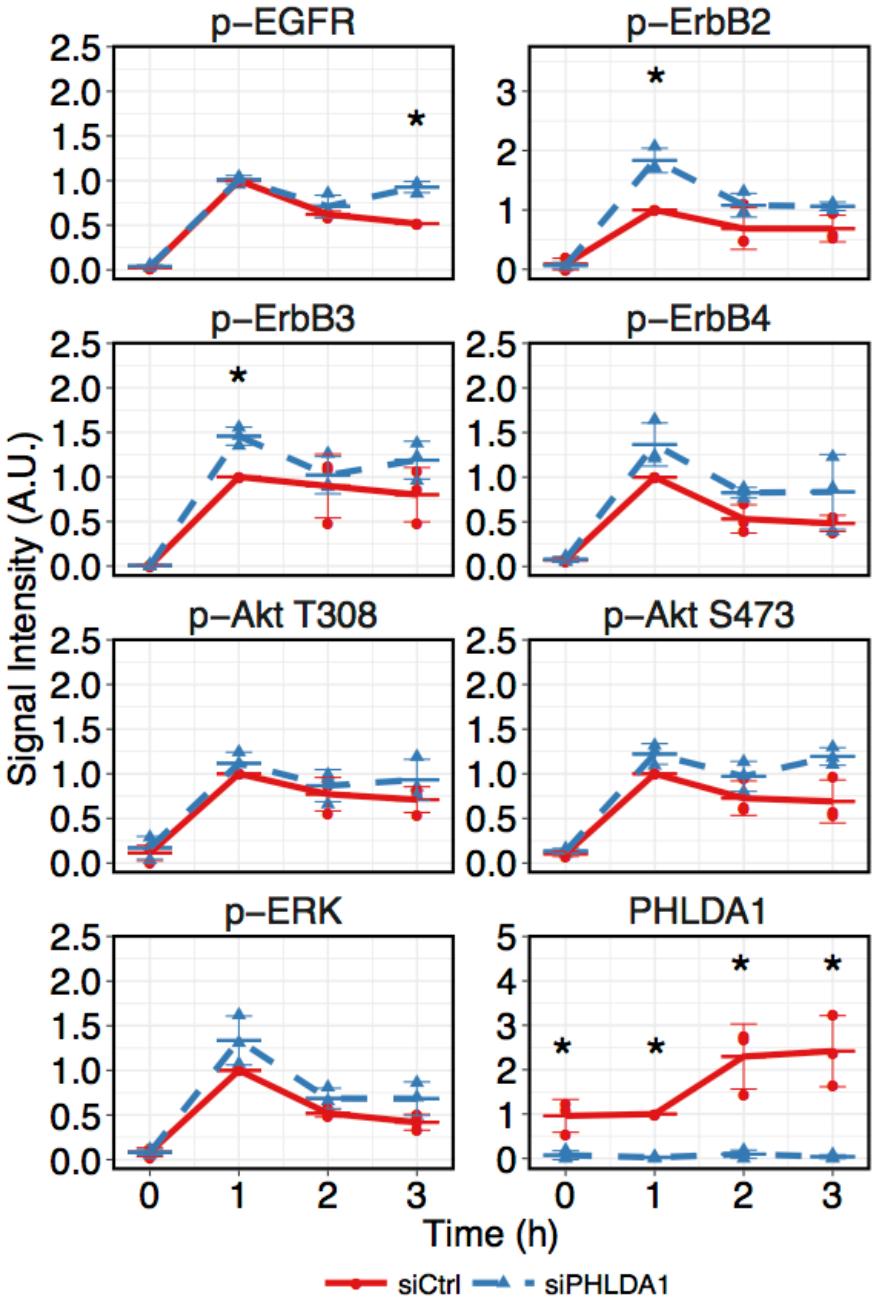

Fig. S4 Quantified value of the blot presented in Fig. 1G. The band intensities of phosphorylated proteins were quantified by dividing by that of total protein, and the band intensities of PHLDA1 were quantified by dividing by that of α-tubulin. Then the values were normalized so that the value of siCtrl sample with HRG treatment for 1 h is designated as 1. Each point represents a result of an independent experiment, and colored bars mean average value of all experiments, and error bars denote standard deviation, n = 3. Two-tailed Welch's test was performed: *, $p < 0.05$.

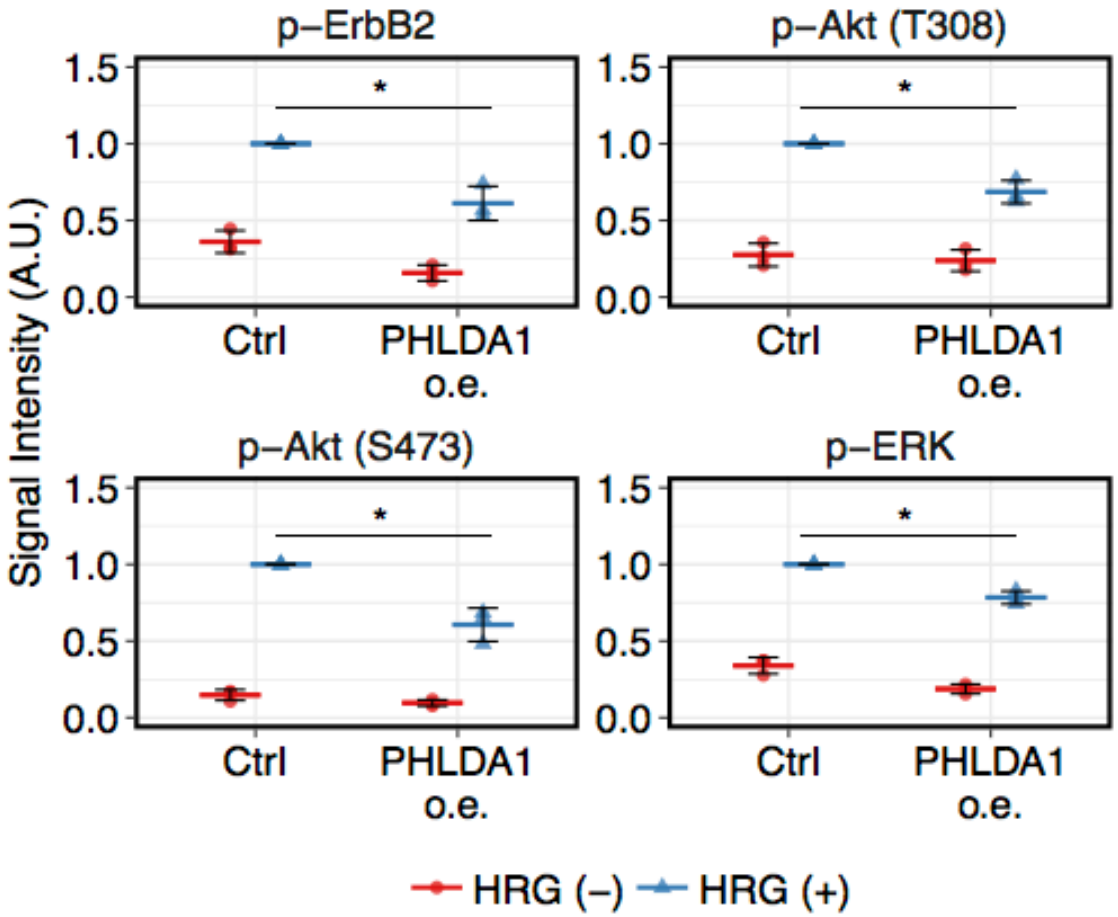

Fig. S5 Quantified value of the blot presented in Fig. 1H. The band intensities of phosphorylated proteins were quantified by dividing by that of total protein, then the values were normalized so that the value of ctrl sample with HRG-stimulated condition is designated as 1. Each point represents a result of an independent experiment, and colored bars mean average value of all experiments, and error bars denote standard deviation, n = 3. Two-tailed Welch's test was performed: *, $p < 0.05$.

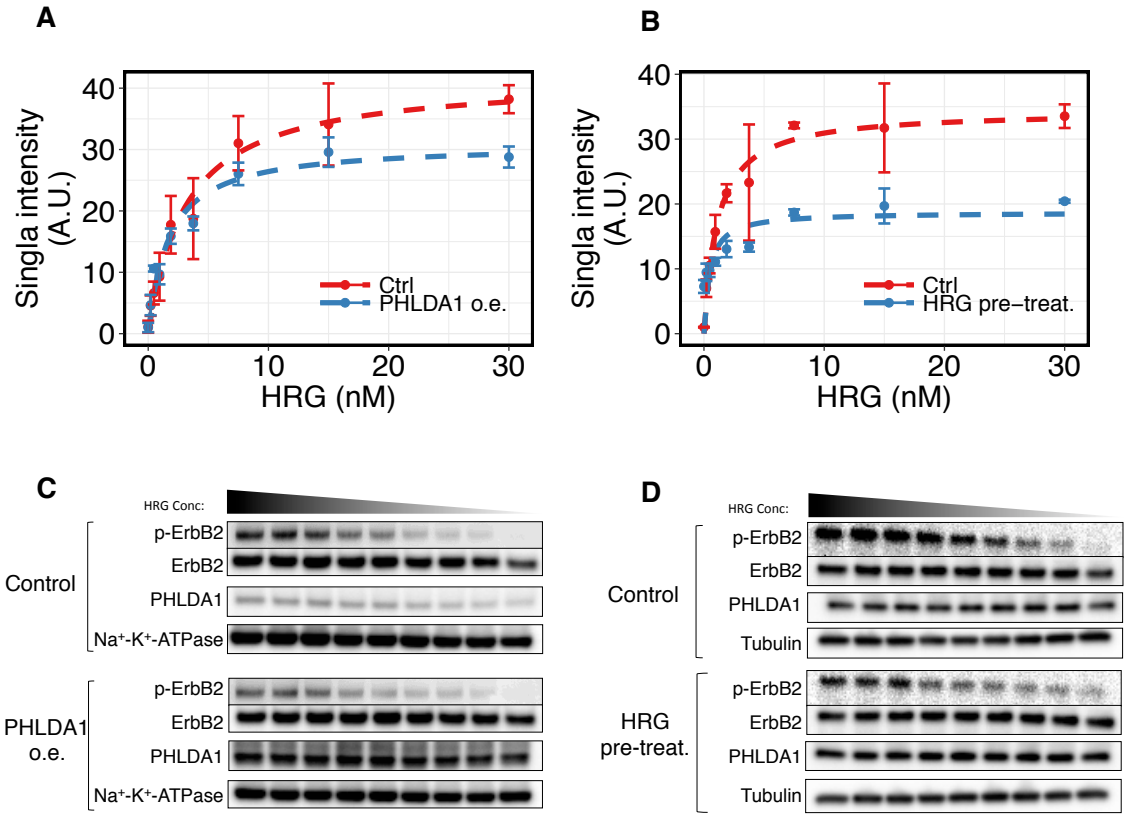

Fig. S6 The effect of PHLDA1 overexpression and HRG pre-treatment on HRG dose response of phospho-ErbB2 ***A***, Effect of PHLDA1 overexpression on ligand dose-dependent ErbB2 receptor phosphorylation in the plasma membrane fraction. ***B***, Effect of HRG pretreatment on ligand dose-dependent ErbB2 receptor phosphorylation. MCF-7 cells were first treated with 1 nM HRG for 3 h, and then a second stimulation for 2 min with different concentrations of HRG. ***C*** and ***D*,** Representative immunoblot data presented in ***A*** and ***B***, respectively. Blots show representative results from one of three experiments.

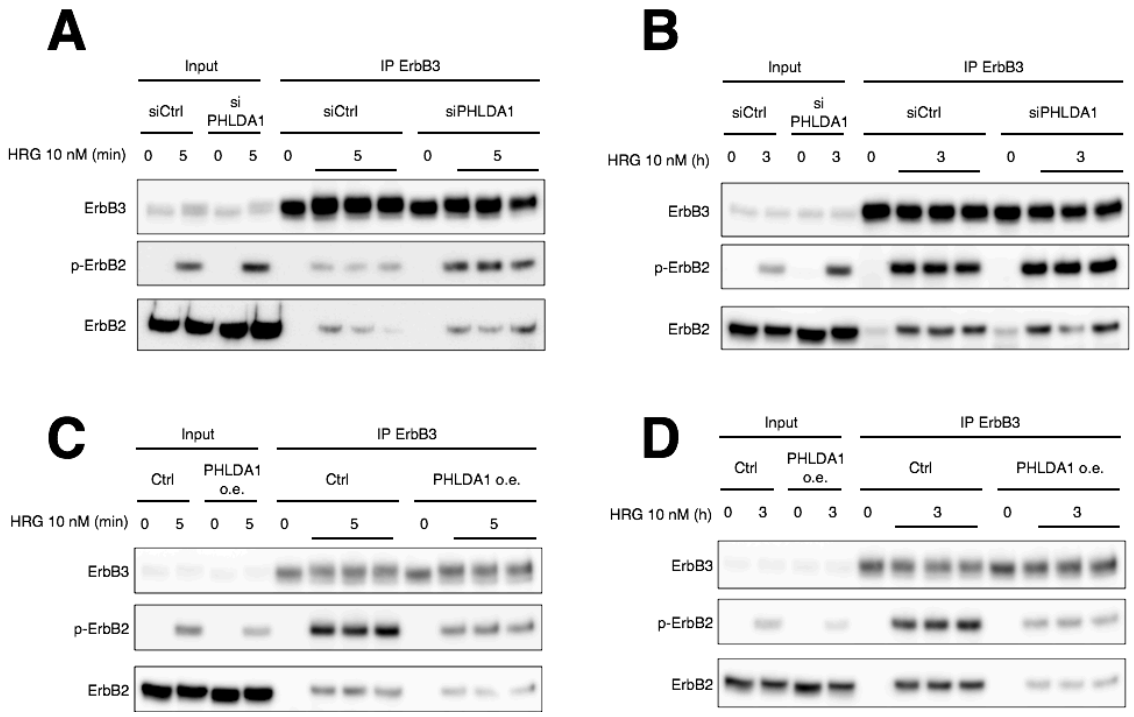

Fig. S7 Representative immunoblot images for the data presented in Fig. 2, **C** to **F**. ***A*** to ***D***, Representative immunoblot images for the data presented in Fig. 2, C to F, respectively.

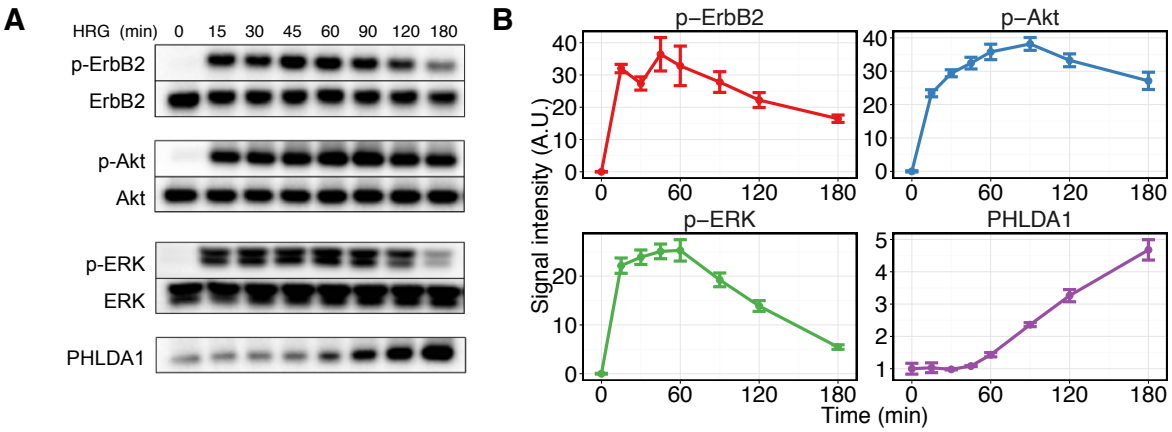

Fig. S8 Time-course experiment of HRG-induced ErbB receptor signaling. Time-course kinetics of protein phosphorylation and total protein after 10 nM HRG administration to MCF-7 cells assessed by western blot. ***A***, Representative immunoblot images of the data. Blots show representative results from one of three experiments. ***B***, Quantified data. Error bars indicate SD in triplicate.

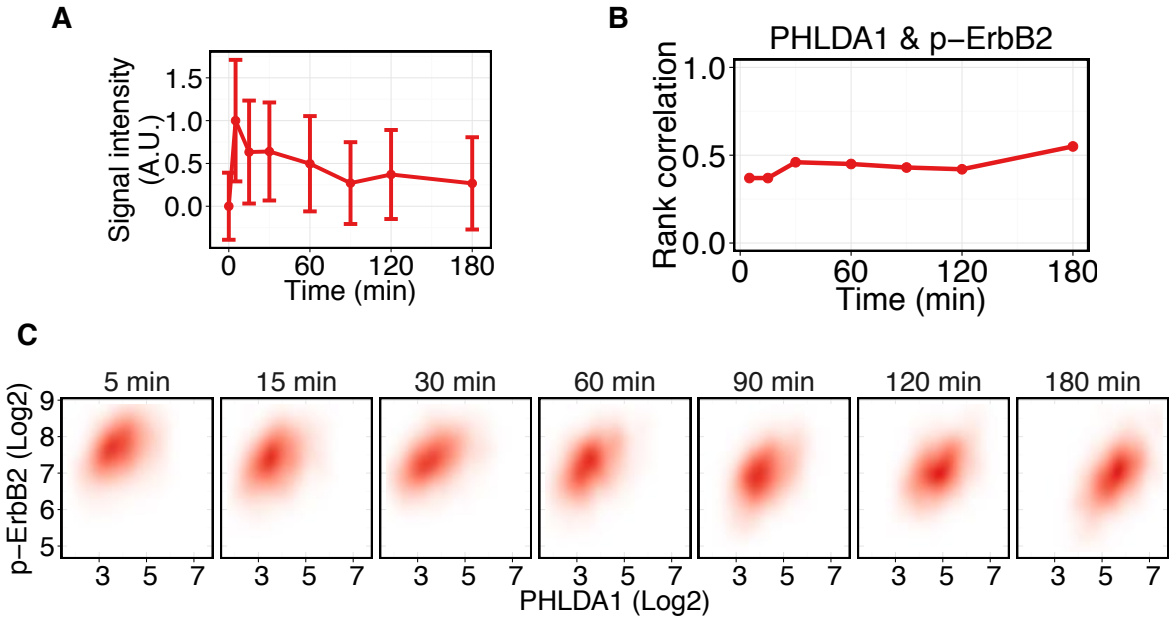

Fig. S9 Confirmation of the time course pattern of phospho-ErbB2 using a different antibody. ***A***, Time-course pattern of phospho-ErbB2 detecting by an imaging cytometer. Quantified data were normalized the same way as Fig. 3A. ***B***, The time-course pattern of Spearman's rank correlation between phospho-ErbB2 and PHLDA1 in a cell population. These data were obtained by using sc-12352-R phospho-ErbB2 antibody (Santa Cruz). ***C***, 2D-probabilistic density of p-ErbB2 and PHLDA1 in a cell population stimulated by 10 nM of HRG. Each panel contains at least 1,500 cells.

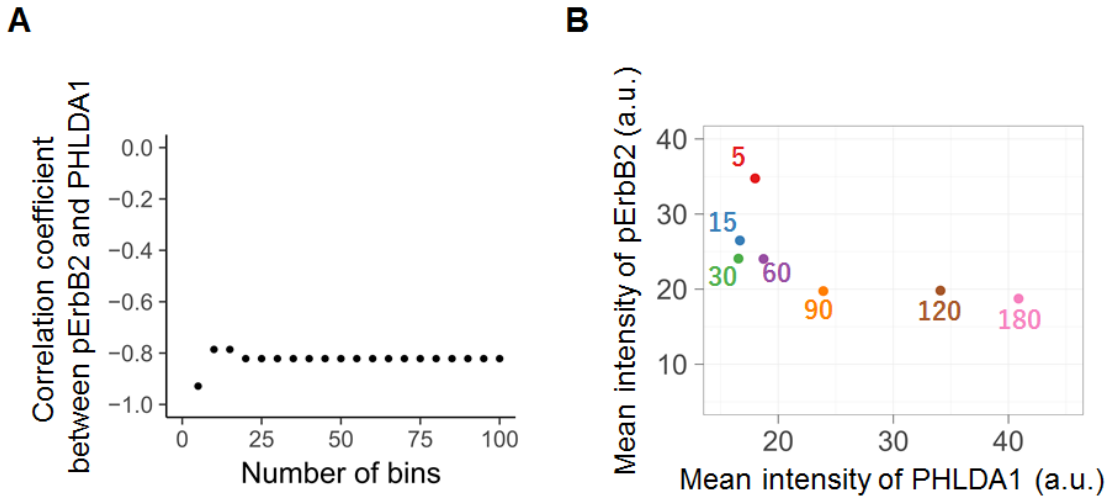

Fig. S10 Validation of the metric "mean expression level per cell". ***A***, Rank correlation coefficients calculated using the mean expressions of pErbB2 and PHLDA1 per cell. The mean expressions per cell were estimated from the histograms of normalized signal intensities of individual cells at each time point for different bin numbers. ***B***, Mean normalized signal intensities of pErbB2 and PHLDA1 at each time point.